

# Curvature Effects on Electron States of Semiconducting Nanotubes

Susumu Okada<sup>1</sup>, Satoshi Ogawa<sup>2</sup>, and Shigeo Maruyama<sup>2</sup>

<sup>1</sup>*Institute of Physics and Center for Computational Physics,  
University of Tsukuba, Tennodai, Tsukuba 305-8571, Japan*

<sup>2</sup>*Department of Mechanical Engineering, The University of Tokyo,  
7-3-1 Hongo, Bunkyo-ku, Tokyo 113-8656, Japan*

(Dated: February 20, 2004)

Based on the generalized tight-binding model we study the electronic structure of all the semiconductor nanotubes with their diameters between 7.5 Å and 15.5 Å. We find that the van Hove peak separations versus nanotube diameters shows a qualitative difference from the well known plot based on zone-folding models. It has been clarified that the top of the valence band of the  $(n, m)$  nanotube in which the remainder of  $|n - m|$  divided 3 is 1 is lower in energy than that of the other semiconducting nanotubes of which remainder is 2. This dependence is originated from the wavefunction characters at the wavenumbers allowed by the periodic boundary condition along the circumference imposed on the hexagonal Brillouin zone of the graphene sheet.

PACS numbers: 73.22.-f, 71.20.Tx, 73.20.At

Carbon nanotubes [1] have attracted a lot of attention in the last decade due to possible applications for nano-meter scale electronic devices in the next generation [2]. One of the most fascinating characteristics is that the nanotubes exhibit interesting variations of their electronic structures depending on their atomic arrangement along the circumference [3–5]. The electronic structures of the nanotubes are characterized by the chiral index  $(n, m)$ : The nanotubes are metallic when  $|n - m|$  is a multiple of three, whereas they are semiconducting otherwise [3, 5]. The peculiar electronic property is due to an anisotropic energy bands of the graphene sheet and an additional boundary condition imposed on electron states of a graphite sheet which is rolled into each nanotube. The electronic property indicates a possibility to identify an atomistic geometry of the nanotube by comparing experimental results on optical spectra for the nanotube. Indeed, a plot of van Hove transition energies versus nanotube diameters, which is called Kataura plot [6], is now a commodity for an experimentalist using resonant Raman spectroscopy. The original Kataura plot was generated by the zone-folding technique based on the  $\pi$  tight-binding energy dispersion of graphene [6]. By the adjustment of the interaction energy  $\gamma_0$ , satisfactory fit to resonant Raman scatterings by individual nanotubes was obtained [7, 8]. On the other hand, the near infrared fluorescence spectra of water-suspended isolated nanotubes measured for scanning excitation wavelength [9] gave first band gap,  $E_{11}$ , and second band gap,  $E_{22}$ , of each nanotube. A tight-binding model including the third nearest neighbor transfer [10] was used for the assignment of  $(n, m)$  to the experimentally observed pairs of  $E_{11}$  and  $E_{22}$ . Unfortunately, the discrepancy of these two major Kataura plots [7, 11] is quite large.

In addition to the chirality, it has been reported that curvature also affects the electronic structure of the nanotubes. In the graphite, electron states are classified into two groups;  $\sigma$  ( $sp^2$  orbital) and  $\pi$  ( $p_z$  orbital) states. In the nanotubes, however, the  $\pi$  states are rehybridized

with the  $\sigma$  states due to its lack of mirror symmetry. Thus the rehybridization causes downward shifts of the  $\pi$  electron states of the nanotubes and the amount of the shift depends on the curvature. This effect induces the metallization for single-walled nanotubes smaller than (6,0) [12, 13] and double walled nanotubes with an inner (7,0) nanotube [14].

There have been a lot of theoretical calculations those studied the electronic structure of the single-walled nanotubes [3–5, 12]. Due to large translational vectors, the quantitative electronic structures of the chiral nanotubes are not sufficiently elucidated yet [13, 15, 16]. However, the quantitative electronic structures of these nanotubes are recently desired to identify the chirality of the nanotubes by comparing the fluorescence spectra observed experimentally, because the dominant chirality of nanotube samples depending on the generation process is now being discussed [17–19]. Thus, in the present work, we study the electronic structures of all semiconducting nanotubes with their diameters ranging from 7.5 Å to 15.5 Å by using the generalized tight-binding model which quantitatively reproduces the electronic structures of various carbon materials. This diameter range covers the diameter of experimentally obtainable single-walled nanotubes by laser-furnace [20], HiPco [21], or alcohol CCVD techniques [22]. In particular, we give detailed discussions for the electron states near the gap,  $E_{11}$  and  $E_{22}$  gaps, which are related to emission and excitation spectra, respectively. Our systematic studies elucidate that the occupied electron states strongly depend not only on the curvature but also on the chiral vectors of the semiconducting nanotubes.

The electronic structures of nanotubes are calculated by using the generalized tight-binding model [23, 24]. Here,  $2s$  and  $2p$  states of a carbon atom are used as the basis set to discuss the  $\pi$ - $\sigma$  rehybridization induced by the curvature of the nanotube. Furthermore, the nonorthogonality of the atomic orbitals between neighboring sites is fully taken into account. Transfer and

overlap integrals between neighboring atomic orbitals have suitable distance dependences in order to reproduce the electronic band structures of various atomic configuration of the carbon atoms. To give the more quantitative discussion for the electronic structure of the nanotubes, we chose the parameter set which gives consistent results with those by the LDA calculation for both graphite and solid C<sub>60</sub> [24]. Indeed, the present model is found to be accurate enough to reproduce the electronic structure of various carbon materials [3, 25].

To obtain the electronic structure of the graphene sheet, we also use the local density approximation (LDA) [26, 27] in the density functional theory (DFT) [28, 29]. Norm-conserving pseudopotentials generated by using the Troullier-Martins scheme are adopted to describe the electron-ion interaction [30, 31]. The valence wave functions are expanded by the plane-wave basis set with a cutoff energy of 50 Ry.

Figure 1 (a) shows the energies which give the first occupied ( $\varepsilon_1$ ), the second occupied ( $\varepsilon_2$ ), the first unoccupied ( $\varepsilon_1^*$ ), and the second unoccupied ( $\varepsilon_2^*$ ) van Hove singularities of semiconducting nanotubes as a function of the tube diameter. The  $\varepsilon_1$  energies are obviously classified into two groups: The tubes possess their indices  $n$  and  $m$  which satisfy the relations  $|n - m| = 3N + 1$  (mod=1 nanotubes) and  $|n - m| = 3N + 2$  (mod=2 nanotubes), where  $N$  are integer numbers. The  $\varepsilon_1$  energies of the mod=1 nanotubes are found to be lower in energy than those of the mod=2 nanotubes possessing the same diameter. The result is in sharp contrast to those obtained by the  $\pi$  only tight-binding calculation (not shown) and by the zone folding analysis to the two-dimensional energy band of graphene sheet calculated in density functional theory [Fig. 1 (b)] and in the generalized tight-binding model [Fig. 1 (c)]. Since the curvature effect is not taken account in the  $\pi$  tight-binding and the zone-folding analysis, this discrepancy elucidates an importance of the curvature for the electronic structures of the semiconducting nanotubes.

In the zone folding analysis, the energies of  $\varepsilon_1$  and  $\varepsilon_1^*$  are determined by the distance between K point where the  $\pi$  band touches the  $\pi^*$  band and the wavenumber allowed by the periodic boundary condition along the circumference of the nanotube which gives a discrete set of the  $k$  lines in the hexagonal Brillouin zone of the graphene sheet. The anisotropic energy bands of  $\pi$  and  $\pi^*$  states around the K point results in the above interpretation: Gradients of  $\pi$  and  $\pi^*$  states along the K- $\Gamma$  line is larger than those along the K-M line (Fig. 2). As shown in Fig. 2, it is found that the distance between K point and one of discretized one-dimensional wavenumbers for the mod=1 tube [K-M direction in Fig. 2 (a)] is the same as that for the mod=2 tube [K- $\Gamma$  direction in Fig. 2 (b)] possessing almost the same diameter. Thus the  $\varepsilon_1$  energy of the mod=2 tube is lower than that of the mod=1 tube due to the large gradient of the  $\pi$  band along the K- $\Gamma$  line. For the single orbital tight binding approximation, since the curvature effects which are de-

scribed by the hybridization between  $2s$  and  $2p$  states of the C atoms are not taken account, the calculation enables us to reach the same conclusion; the  $\varepsilon_1$  of the mod=2 tube is lower than that of the mod=1 tube.

The result obtained by the above procedures is not in the case for the calculations which take account of the modulation of the electronic structures originated from the curvature of the nanotubes, e.g. the generalized tight-binding model and DFT calculations. In these cases, due to their lack of the mirror symmetry at the atomic array, the  $\pi$  states are rehybridized with the  $\sigma$  state. The rehybridization causes downward shifts of the  $\pi$  electron states of the nanotubes and the amount of the shift depends on the curvature, since the  $\sigma$  state possesses lower energy than the  $\pi$  states. It is obvious that the downward shift for the tube with small diameter is larger than those for the thicker tubes, because the rehybridized  $\pi$  states contains the substantial amount of  $\sigma$  components. Furthermore, it is found that the downward shift depends not only on the curvature but also on the chiral index of the nanotube.

Figure 3 shows the squared wavefunction of the  $\pi$  state of the graphene sheet at  $\Gamma$  and M points calculated by the LDA. The wavefunction is found to possess antibonding character at the M point whereas bonding character at the  $\Gamma$  point. The result indicates that the downward shift of the  $\pi$  state depends on the wavenumbers  $k$  allowed by the periodic boundary condition imposed on the tubular structure: In the mod=1 tube, the wavenumber which gives the top of the valence band is located near the K-M line [Fig. 2 (a)]. Along the line, the  $\pi$  state possesses antibonding character which is not affected by the rehybridization of the  $\pi$  and  $\sigma$  states so that the downward shift of the state takes place. On the other hand, in the mod=2 tubes, the wavenumber corresponding to the valence-band top is located near the K- $\Gamma$  line [Fig. 2 (b)] on which the  $\pi$  state exhibits bonding character. This distribution of the state strongly affects the energy value of  $\varepsilon_1$  because the rehybridization induces the modulation of the wavefunction distribution which costs the electron energy. Thus the  $\varepsilon_1$  energy shifts upward compared with that of the mod=1 tube. Owing to the difference in the direction of the wavenumber giving the  $\varepsilon_1$  energy, the electronic structures around the energy gap for the semiconducting nanotubes exhibit different characteristics from those obtained by the  $\pi$  tight-binding calculation and the zone-folding analysis on the graphene sheet.

In addition to the  $\varepsilon_1$ , the energy  $\varepsilon_2$  also exhibits the opposite nature to those obtained by the  $\pi$  tight-binding calculation and the zone-folding analysis. In the case, the wavenumbers which give the  $\varepsilon_2$  are located near the K- $\Gamma$  and K-M lines for mod=1 and mod=2 tubes, respectively. Thus, the  $\varepsilon_2$  of the mod=1 tubes substantially shift upward and possess higher energy than those of the mod=2 tubes.

Based on the calculations, we replot a new Kataura plot that gives the energies  $E_{11} = \varepsilon_1^* - \varepsilon_1$  and  $E_{22} = \varepsilon_2^* - \varepsilon_2$  as a function of the tube diameter. Due to the

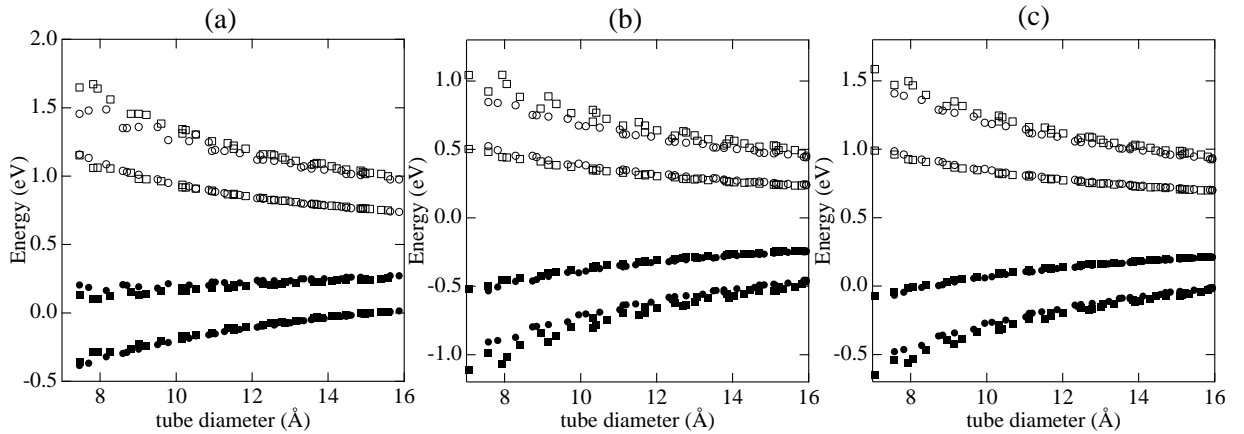


FIG. 1: Energies of  $\varepsilon_1$ ,  $\varepsilon_1^*$ ,  $\varepsilon_2$ , and  $\varepsilon_2^*$  for semiconducting nanotubes as a function of the tube diameter obtained by using (a) the generalized tight-binding model, and zone-folding analysis for the electronic energy band of the graphene sheet calculated by (b) the density functional theory and (c) the generalized tight-binding model. Squares and circles denote the mod=1 and mod=2 tubes, respectively. Solid and empty marks for each tube denote occupied ( $\varepsilon_1$  and  $\varepsilon_2$ ) and unoccupied ( $\varepsilon_1^*$  and  $\varepsilon_2^*$ ) electron states, respectively. In (b), the energies are measured from the Fermi level of the graphene sheet.

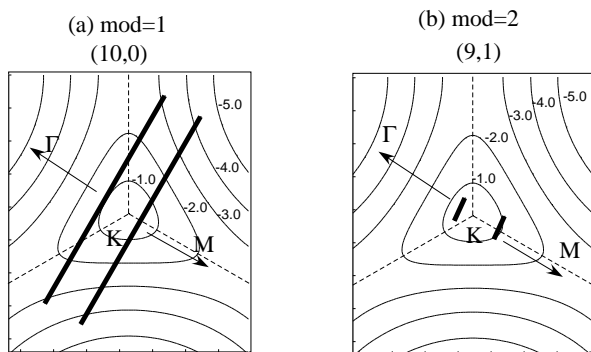


FIG. 2: The wavenumbers  $k$  allowed by the periodic boundary condition along the circumference for (a) the mod=1 tube, (10,0) and (b) the mod=2 tube, (9,1) near K point in the hexagonal Brillouin zone of the graphene sheet. Thick solid and dotted lines denote wavenumbers  $k$  around the K point and the boundary of the first Brillouin zone of the graphene sheet, respectively. Contour lines denote the two-dimensional energy band of the graphene sheet calculated by LDA. The values shown in figure are in the unit of eV.

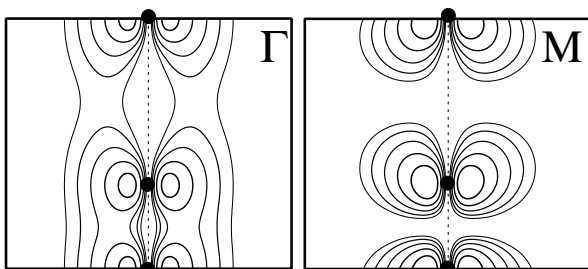


FIG. 3: Contour plots of the squared wavefunction of the  $\pi$  state of the graphene sheet at  $\Gamma$  and M points. Each contour represents twice (or half) the density of the adjacent contour lines. Solid circles and dashed line denote the C atoms and the position of the graphene sheet, respectively.

asymmetric behaviour of the  $\varepsilon_1$  and  $\varepsilon_2$  for the mod=1 and the mod=2 tubes with the same diameter, the gap energy  $E_{11}$  and  $E_{22}$  of the mod=1 tube is larger than that of the mod=2 tube. The results open a possibility of new assignment for the diameter of the nanotubes by comparing the optical spectra corresponding to the gaps  $E_{11}$  and  $E_{22}$ . As shown in Fig. 4, the energy difference between the energy gaps of the mod=1 and mod=2 tubes is substantially small. The small dispersion of the gap energy is due to the localized nature of the basis set for the calculation in which we only take account of the atomic orbitals of the  $2s$  and the  $2p$  states of C atom. In this case, the localized states are insufficient to describe the rehybridization effects on the  $\pi$  and  $\sigma$  states for the tubes with substantial curvature. It is expected that the dispersion of the gap energies are underestimated in the present calculation and that the calculations in which the basis set sufficiently expresses the extended nature of the wavefunction, e.g. the LDA [16], the generalized gradient approximation, and the quasi particle approximation [32], give larger dispersion for the gap energies. We thus conclude that further calculations are desired to obtain the ultimate version of the Kataura plot.

In summary, based on the generalized tight-binding calculations we explored the electronic structures of all the semiconducting nanotubes with their diameters between 7.5 Å and 15.5 Å. We found that the occupied electron states strongly depends not only on the curvature but also on the chiral vector of the nanotubes. The highest occupied states of the mod=1 nanotube is lower in energy than that of the mod=2 nanotube with the same diameter. While the energy which gives the second occupied van Hove singularity of the mod=1 tube is higher than that of the mod=2 tube. The peculiar chirality dependence of the  $\pi$  electron states is totally due to the distribution of the wavefunction at the wavenumbers

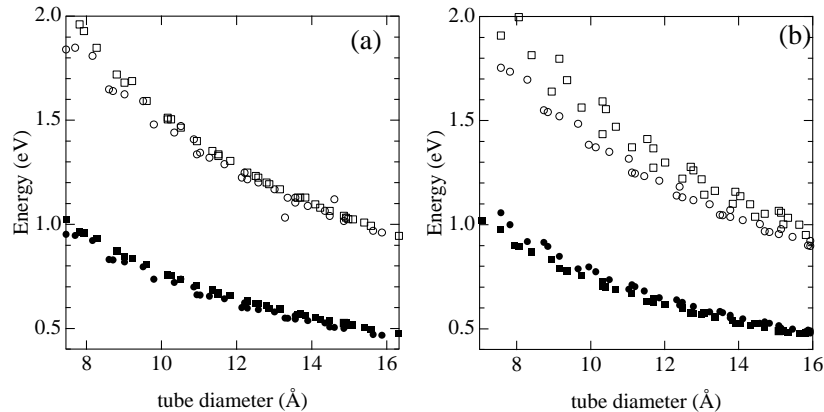


FIG. 4: Energy gap between the first occupied and unoccupied van Hove singularity ( $E_{11}$ ) of the semiconductor nanotubes as a function of the tube diameter obtained by (a) the generalized tight-binding model and (b) zone-folding analysis for the electronic energy band of the graphene sheet calculated by LDA. Energy gap between the second occupied and unoccupied van Hove singularity ( $E_{22}$ ) is also shown. Squares and circles denote the mod=1 and mod=2 tubes, respectively. Solid and empty marks for each tube denote the  $E_{11}$  and  $E_{22}$ , respectively.

corresponding to the states. The curvature induces the rehybridization between  $\pi$  and  $\sigma$  states resulting in the modulation of the distribution of the wavefunctions. On the K- $\Gamma$  line, the modulation causes the upward shift of the electron states due to the bonding character of the wavefunction along this line. On the other hand, on the K-M line, the electron state is not affected due to the antibonding character of the wavefunction. Owing to the effects, the energy gap between the first occupied and unoccupied van Hove singularities for the mod=1 tube is

larger than that of the mod=2 tube.

We thank N. Hamada for providing the tight-binding program used in this work. We benefited from fruitful conversations with T. Miyake. This work was partly supported by ACT-JST (Japan Science and Technology Corporation), Special Research Project on Nanoscience in University of Tsukuba, NEDO under the Nanotechnology Materials Program, and Grant-in-Aid for Scientific Research from Ministry of Education, Science, and Culture of Japan.

- 
- [1] S. Iijima, *Nature*, **354**, 56 (1991).
  - [2] S. J. Tans, A. R. M. Verschueren, and C. Dekker, *Nature (London)*, **393**, 49 (1998).
  - [3] N. Hamada, S. Sawada, and A. Oshiyama, *Phys. Rev. Lett.* **68**, 1579 (1992).
  - [4] J. W. Mintmire, B. I. Dunlap, and C. T. White, *Phys. Rev. Lett.*, **68**, 631 (1992)
  - [5] R. Saito, *et al.*, *Appl. Phys. Lett.* **60**, 2204 (1992).
  - [6] H. Kataura, *et al.*, *Synth. Met.* **103**, 2555 (1999).
  - [7] R. Saito, G. Dresselhaus, and M. S. Dresselhaus, *Phys. Rev. B* **61**, 2981 (2000).
  - [8] A. Jorio, *et al.*, *Phys. Rev. Lett.* **86**, 1118 (2001).
  - [9] S. M. Bachilo, *et al.*, *Science*, **298**, 2361 (2002).
  - [10] S. Reich, *et al.*, *Phys. Rev. B* **66**, 035412 (2002).
  - [11] R. B. Weisman and S. M. Bachilo, *NanoLetters*, **3**, 1235 (2003).
  - [12] X. Blase, *et al.*, *Phys. Rev. Lett.*, **72**, 1878 (1994).
  - [13] Z. M. Li, *et al.*, *Phys. Rev. Lett.*, **87**, 127401 (2001).
  - [14] S. Okada and A. Oshiyama, *Phys. Rev. Lett.*, **91**, 216801 (2003).
  - [15] I. Cabria, J. W. Mintmire, and C. T. White, *Phys. Rev. B* **67**, 121406 (2003).
  - [16] Y. Akai, *et al.*, in Abstracts of The 26th Fullerene-Nanotubes General Symposium, p. 49, 2004 (Fullerene-Nanotubes Research Association, Nagoya).
  - [17] S. M. Bachilo, *et al.*, *J. Am. Chem. Soc.*, **125** 11186 (2003).
  - [18] S. Maruyama, *et al.*, *New J. Phys.*, **5**, 149 (2003).
  - [19] Y. Miyauchi, *et al.*, *Chem. Phys. Lett.*, (2004), in press.
  - [20] A. Thess, *et al.*, *Science*, **273**, 483 (1996).
  - [21] M. J. Bronikowski, *et al.*, *J. Vac. Sci. Technol. A* **19**, 1800 (2001).
  - [22] S. Maruyama, *et al.*, *Chem. Phys. Lett.* **360**, 229 (2002).
  - [23] N. Hamada, unpublished.
  - [24] S. Okada and S. Saito, *J. Phys. Soc. Japan*, **64**, 2100 (1995).
  - [25] S. Saito, *et al.*, *Phys. Rev. Lett.*, **75**, 685 (1995).
  - [26] J. P. Perdew and A. Zunger, *Phys. Rev. B* **23**, 5048 (1981).
  - [27] D. M. Ceperley and B. J. Alder, *Phys. Rev. Lett.* **45**, 566 (1980).
  - [28] P. Hohenberg and W. Kohn, *Phys. Rev.* **136**, B864 (1964).
  - [29] W. Kohn and L. J. Sham, *Phys. Rev.* **140**, A1133 (1965).
  - [30] N. Troullier and J. L. Martins, *Phys. Rev. B* **43**, 1993 (1991).
  - [31] L. Kleinman and D. M. Bylander, *Phys. Rev. Lett.* **48**, 1425 (1982).
  - [32] T. Miyake and S. Saito, *Phys. Rev. B* **68**, 155424 (2003).